

# Templating and Replication of Spiral Photonic Crystals for Silicon Photonics

Kock Khuen Seet, Vygantas Mizeikis, Kenta Kannari, Saulius Juodkazis, Hiroaki Misawa, Nicolas Tétreault, and Sajeev John

(Invited Paper)

**Abstract**—This paper describes femtosecond laser lithography of 3-D photonic crystal templates in commercial photoresist SU-8 and replication of these templates with silicon. Using this approach, silicon-based photonic crystals having 3-D square spiral architecture and exhibiting photonic stop gaps near the 2.5- $\mu\text{m}$  wavelength were fabricated. Possibilities to use a multiple-beam interference technique for two-photon absorption templating of photonic crystals are explored.

**Index Terms**—Femtosecond laser lithography, photonic band gap materials, silicon.

## I. INTRODUCTION

THREE-DIMENSIONAL (3-D) micro- and nanostructuring of semiconductors is of tremendous importance to the development of integrated electronic, optical, mechanical, fluidic, or hybrid circuits. Currently, spatially periodic 3-D semiconductor microstructures attract strong interest due to their applicability as photonic band gap (PBG) materials, or photonic crystals (PhC) [1], [2]. High refractive index semiconductors are particularly attractive for the fabrication of PhC structures, because they enable to achieve high index contrast, and favor opening of spectrally wide PBGs. Despite the nanometric accuracy provided by the currently available semiconductor fabrication techniques, their use for genuine 3-D structuring of semiconductors is problematic. Thus, extended 3-D semiconductor-based PhCs can only be generated via painstaking and costly processes of layer-by-layer growth and planar structuring [3]–[5]. These difficulties have fueled the search for easier and more effective approaches to the creation of 3-D high refractive index semiconductor structures. One of the most popular approaches employs

the so-called template inversion method, where a periodic template is fabricated at first from low refractive index materials using techniques better suited for the formation of 3-D periodic structures. Subsequently, air cavities of the template are infiltrated, first by a heat-resistant sacrificial material, and then by a high refractive index semiconductor using chemical vapor deposition (CVD) or other suitable process. The templates are optionally removed by thermal or chemical means. The final structure replicates the spatial periodicity of the starting template, while its refractive index contrast becomes enhanced, leading to the opening of a 3-D PBG. For instance, silicon infiltration into 3-D artificial opal PhC structures was confirmed to lead to the opening of a complete PBG [6]. Recently, a new class of PhC structures with square spiral architecture was proposed, in which spectrally wide and structurally robust PBG can open, provided that the constituent spirals have a high refractive index, close to that of silicon ( $n_{\text{Si}} = 3.4$ ) [7], [8]. This kind of 3-D architecture can be fabricated directly from Si using the glancing-angle deposition (GLAD) technique [9]–[12]. The class of spiral architecture also includes circular spiral structures [13], which cannot be fabricated even by the GLAD technique. Previously, we have demonstrated high flexibility of a 3-D laser lithography technique known as direct laser writing (DLW) for the fabrication of high-quality 3-D periodic woodpile [14], [15], square spiral [16], [17], and circular spiral [18] architectures in commercially available low refractive index photoresist SU-8. The achievable spatial resolution of DLW in SU-8 has already passed the  $\sim 100$  nm limit [19]. Another implementation of laser lithography allows simultaneous recording of large 3-D samples using periodic intensity patterns resulting from multiple-beam interference, or from transmission through a phase mask [20]. The interference (or holographic) recording method allows realization of PhC structures with periodic symmetries favorable for the opening of spectrally-wide and structurally-robust PBGs, provided that sufficient index contrast is achieved by infiltration [21], [22].

Availability of these versatile 3-D PhC templating techniques was recently supplemented by the procedure for template infiltration by high refractive index materials. Silicon replication of SU-8 templates having 3-D woodpile architecture was successfully conducted and a PBG in the structure was confirmed [23]. The same approach was also successfully used for the fabrication of 2-D silicon photonic quasicrystals [24]. Availability of infiltration inversion techniques enhances strongly the applicability of low-index 3-D templates fabricated by laser lithography. In this paper, we describe templating of 3-D spiral

Manuscript received December 10, 2007; revised February 4, 2008. This work was supported by the Ministry of Education, Culture, Sports, Science, and Technology of Japan under KAKENHI Grant-in-Aid 470 for Scientific Research on the Priority Area “Strong Photons-Molecules Coupling Fields.” The work of N. Tétreault was supported by the F.E. Beamish Graduate Scholarship (OGSST). The work of S. John was supported by the Natural Sciences and Engineering Research Council of Canada.

K. K. Seet, V. Mizeikis, K. Kannari, S. Juodkazis, and H. Misawa are with Hokkaido University, Sapporo 001-0021, Japan (e-mail: himawari@es.hokudai.ac.jp; vm@es.hokudai.ac.jp; kannari@es.hokudai.ac.jp; saulius@es.hokudai.ac.jp; misawa@es.hokudai.ac.jp).

N. Tétreault was with the University of Toronto, Toronto ON M5S 1A7, Canada. He is now with the University of Cambridge, Cambridge CB3 0FF, U.K. (e-mail: nt271@cam.ac.uk).

S. John is with the University of Toronto, Toronto ON M5S 1A7, Canada (e-mail: john@physics.utoronto.ca).

Color versions of one or more of the figures in this paper are available online at <http://ieeexplore.ieee.org>.

Digital Object Identifier 10.1109/JSTQE.2008.922909

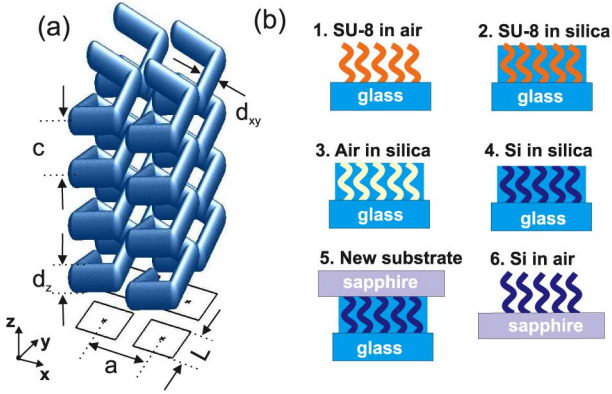


Fig. 1. Schematic illustration of the square spiral PhC architecture and definition of its (a) main parameters and (b) the main steps of double-inversion process of SU-8 templates by silicon.

PhC structures in SU-8 using the DLW technique, and report optical properties of the PhC structures obtained from these templates by double-infiltration of silica glass and silicon. The SU-8 templates and final samples were found to exhibit signatures of photonic stop gaps (PSG) in reflection spectra at infrared wavelengths of 1.6 and 2.5  $\mu\text{m}$ , respectively. These findings agree well with theoretical estimates deduced from numerically modeled photonic band diagrams and optical reflection spectra. This paper also presents preliminary data on the application of a two-photon absorption (TPA) multiple-beam interference recording technique for the fabrication of high-resolution templates of 3-D PhC structures. Most previous studies [25]–[27] have focussed on single-photon absorption multibeam interference, leading to structures with very small lattice constants. The TPA may be crucial in newly proposed techniques such as optical phase mask lithography [20] in order to achieve a PBG centered at wavelengths near 1.5  $\mu\text{m}$  in silicon after inversion of the polymer template. It is hoped that the reported results will be a step toward practical tailoring of silicon-based PhCs with 3-D spiral architecture and for the holographic TPA recording of PhC templates with the same lateral and axial lattice constants.

## II. FABRICATION OF TEMPLATES AND REPLICATION BY SILICON

### A. Square Spiral Photonic Crystal Architecture

The architecture of 3-D spiral photonic crystal and its main-parameters are explained schematically in Fig. 1(a). Extensive description of this architecture and its various derivatives can be found in the existing literature [7], [8], [13], [28]. Here, we concentrate on the properties of spiral structures categorized as the class of 001-diamond:1 [7], which consists of square spirals arranged on a square lattice on the  $x-y$  plane, and having the arms winding along the  $z$ -axis direction. On the  $x-y$  plane, projection of a spiral arm has the length of  $L$ , while period of the square lattice is  $a$ . Unlike in the original proposal in which spiral arms have circular or rectangular cross sections [7], our structures have elliptical cross section elongated in the  $z$ -axis direction. The elongation coincides with the

propagation direction of the tightly focused laser beam during the DLW fabrication. Elongation of the focal region can be described by the ratio between the longitudinal and lateral diameters of the ellipse,  $d_z/d_{xy}$ , which under our experimental conditions, acquires the value of  $\approx 2.8$ . This circumstance will be discussed next. The fabricated SU-8 templates had parameters  $a = 1.0 \mu\text{m}$ ,  $L = 0.7a$ , and  $c = 1.34a$ . SU-8 templates intended for subsequent inversion by silicon could not be inspected by scanning electron microscopy (SEM), as the latter requires coating of the dielectric structures by metallic Pt|Pd, which would undermine the quality of inversion process. Therefore, the size of the spiral arms could not be determined precisely, but most likely,  $d_{xy} = 0.2 - 0.3 \mu\text{m}$  and  $d_z/d_{xy} \approx 2.8$  were maintained in all fabricated samples.

The procedure of SU-8 template double-inversion by silicon [23] is shown schematically in Fig. 1(b). Air voids of the original SU-8 template (1) are at first completely infiltrated by silica glass ( $\text{SiO}_2$ ) using a low-temperature atmospheric pressure chemical vapor deposition (CVD) process (2). The low-temperature process is necessary in order to avoid degradation of SU-8 which occurs at temperatures above 380  $^\circ\text{C}$ . Then, excessive layers of silica are etched out from the top of the structure using reactive-ion etching (RIE) till the top portion of SU-8 filled features is exposed (not shown in the figure). SU-8 is subsequently removed by etching in  $\text{O}_2$  plasma for more than 20 h, or by calcination in air at a temperature above 450  $^\circ\text{C}$  for more than 6 h. The inversion leads to formation of air voids in silica (3). Additional moderate infiltration of silica into the voids may be used after this step in order to reduce the diameter of voids, and ultimately, of silicon rods (not shown). Next, infiltration of Si into the voids is done through a low-pressure CVD using disilane  $\text{Si}_2\text{H}_6$  as a precursor. At the end of this procedure, silicon features embedded into glass matrix are obtained (4). In this paper, infiltration of the samples was finished at this step. One may optionally continue the inversion process by attaching a new sapphire substrate (5) and removing the glass (both the old substrate and the CVD-deposited glass) by wet etching.

### B. Direct Laser Writing

Optical setup used for the template recording by DLW technique [29] is shown schematically in Fig. 2(a). The light source is a femtosecond Hurricane X system (from Spectra-Physics) with  $\tau_{\text{pulse}} = 130 \text{ fs}$ ,  $\lambda_{\text{laser}} = 800 \text{ nm}$ , repetition frequency adjustable from single shots to 1 kHz, and diameter of a Gaussian beam of about 4 mm (FWHM). The beam intensity is attenuated by a variable attenuator, and divergency compensated by an optical telescope (not shown). Subsequently, the laser beam is coupled into an inverted optical microscope (Olympus IX71) that houses the sample and most of the necessary optical, electrical and mechanical components. The beam is reflected by the dielectric mirror  $D$  highly reflective at  $\lambda_{\text{laser}}$ , and is focused into the sample by a microscope objective lens. The microscope is equipped with an oil-immersion lens having a numerical aperture (NA) of 1.35 and a magnification factor of 100 times. Using such a lens, aberration-free focusing

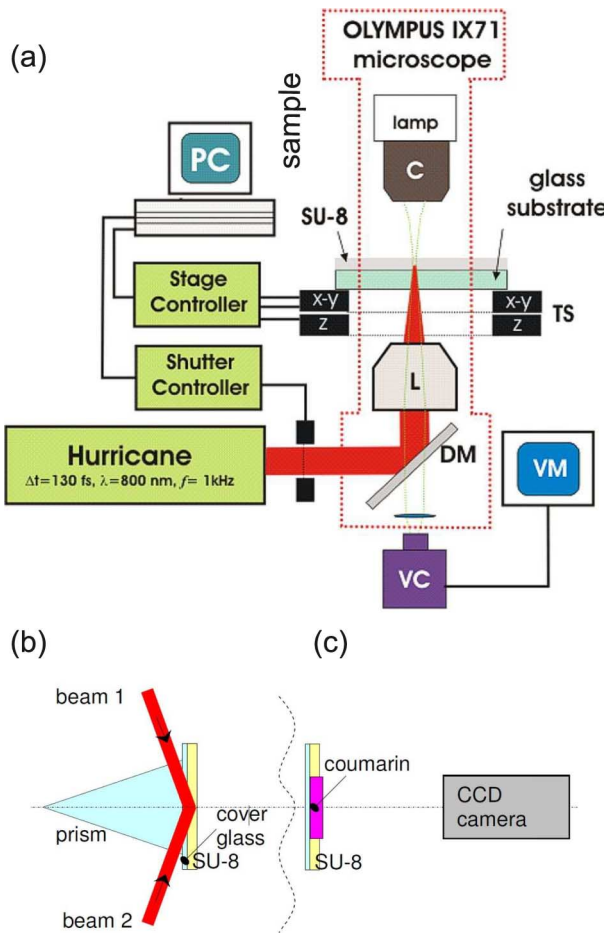


Fig. 2. Optical setups for recording of 3-D PhC templates by (a) DLW and (b) and (c) interference recording techniques.

of a monochromatic plane wave would correspond to the beam diameter at the waist (estimated at the  $1/e^2$  level of peak intensity) of  $w_0 = 1.22\lambda/\text{NA} \simeq 0.723 \mu\text{m}$ . This estimate indicates the approximate resolution of the DLW process. To facilitate writing of continuous features in 3-D, the samples were attached to a high-precision piezoelectric transducer (PZT) controlled 3-D translation stage mounted on the microscope ( $y$ - $y$  and  $z$  stages P-517.2CL and P-518.ZCL, respectively, from Physik Instrumente). The stage provides a maximum positioning range of up to  $100 \mu\text{m}$  and an accuracy of several nanometers. The samples are illuminated by a spectrally filtered light of a halogen lamp using a condenser  $C$ , and can be monitored in transmission within the spectral transparency range of the dielectric mirror  $D$  (visible wavelengths) using a video camera VC and monitor VM. For a properly chosen laser beam intensity, single-photon absorption is negligible, and laser pulses can be delivered into the bulk of the samples without absorptive losses. At the focal region, where local intensity is highest, nonlinear absorption is induced locally, and exposure of SU-8 results. The photomodification is latent, and only at higher exposure doses (below the optical damage threshold), a small local index change, tentatively of the order of  $10^{-4}$ – $10^{-3}$ , is induced by single pulses, resulting in the appearance of small bright or

dark spots. These visual signatures may be useful for *in situ* monitoring of the DLW progress. A personal computer controls the motion of translation stage and a mechanical beam shutter, ensuring that laser pulses irradiate predefined positions in the sample. The samples are recorded in a spiral-by-spiral order.

### C. Processing of the Samples

The samples used for the recording of initial templates were thin films of SU-8, formulation 2002 (from Microchem), deposited on glass substrates by spin-coating. The thickness of the SU-8 films varied from sample to sample, but typically was kept up to  $25 \mu\text{m}$ . Under intense excitation, SU-8, which is nearly completely transparent at the laser wavelength (800 nm), exhibits nonlinear absorption that is ascribed to TPA [30]. The nonlinear absorption, heating [31], and postexposure thermal treatment lead to polymer cross-linking, thus rendering SU-8 insoluble during the subsequent wet development, which dissolves and removes only the unexposed regions. After exposure, the samples were postbaked at  $65^\circ$  for 1 min and at  $95^\circ$  for 5 min for the fixation of cross-linking. Then, development in a propylene glycol methyl ether acetate (PGMEA) developer for 1–5 min. and rinse in iso-propanol for 0.5 min were applied.

The main steps of the double-inversion process of SU-8 templates were already described in Fig. 1(b) and the accompanying discussion. The inversion techniques were essentially the same as reported earlier [23]. However, in our case, the procedures terminated on step (4) in Fig. 1(b), i.e., silica glass was not removed from the structures after silicon infiltration. The resulting samples therefore consist of silicon square spirals (with refractive index  $n_{\text{Si}} = 3.4$ ) embedded in silica glass (refractive index  $n_{\text{SiO}_2} = 1.47$ ). Compared to the equivalent silicon-in-air structures, our samples have slightly lower contrast of the refractive index, but their mechanical robustness is improved. Unfortunately, the presence of glass matrix makes impossible imaging of the samples by SEM, and diameters of the spiral arms cannot be determined straightforwardly.

### D. Recording by Two-Photon-Absorption in Multiple Beam Interference

Interference (or holographic) recording using two-photon absorption (TPA) was carried out using the same 800-nm laser source described in the previous section. Multiple coherent laser beams were obtained from a single input beam by diffraction in a diffractive beam splitter (DBS). The beams propagating at various angles were subsequently collimated by a lens, and passed through a selector (amplitude mask with holes through which only the required beams are transmitted). In our experiments, four beams were selected and overlapped on the sample at a large mutual angle of  $140^\circ$  in order to obtain short-period light intensity patterns. In the sample, the interference pattern creates a corresponding photoexposure pattern. Up to now, 1D and 2D patterns of square lattice were obtained by interference of two and four beams, respectively. Temporal overlap between the beams was ensured with precision of approximately 20 fs using optical variable-delay lines. Holographic recording with

high resolution requires large angles of interference and of incidence on the samples' surface. However, light refraction at the air-photoresist interface prevents coupling of the optical radiation into the sample at incidence angles exceeding the critical angle for total internal reflection. To overcome this limitation, we have adopted the approach known from the literature [25]. Fig. 2(b) shows schematically a simplified 2-D view of the setup. Its main element is the four-sided prism with base angle of  $(70 \pm 1)^\circ$  (shown as a triangle in the sketch), attached to the surface of SU-8 film. The use of prism relaxes the critical angle limitation and allows coupling of four beams into the film of SU-8 at high angles, as shown in the figure. Index matching at the interface between the prism and the sample was ensured by using immersion-oil. The sample-to-prism contact via immersion-oil facilitated translation of sample between exposures without alteration of the space-time alignment of beams.

Operation of this recording scheme depends crucially on the spatial and temporal overlap between the four ultrashort laser pulses. The overlap was verified using a drop of a coumarin dye solution placed on a cover glass right to the SU-8 film, which was spin-coated on the cover glass substrate. The sample was attached on the prism using a drop of a refractive index matched immersion oil. By monitoring the intensity of TPA-excited photoluminescence (PL) on a charge-coupled device (CCD) camera [Fig. 2(c)], a space-time alignment of beams was carried out. The alignment was adjusted by maximizing the nonlinear PL intensity, which directly represents the instantaneous incident power. After the beam alignment, the sample was slid on the immersion-oil into a new position, where the SU-8 film was set at the focus for exposure.

### III. RESULTS AND DISCUSSION

#### A. Structural Properties of Silicon Square Spiral Structures

As mentioned in Section II-A, the SU-8 templates belong to the category of [001]-diamond:1 structures having  $L < a$ . The fabricated structures have design parameters of  $a = 1.0 \mu\text{m}$ ,  $L = 0.7a$ , and  $c = 1.34a$ . These parameters are controlled with accuracy of a few nanometers during the fabrication, and as evidenced by our earlier papers dealing with fabrication of similar structures in SU-8, shrinkage or deformation of the samples after their development is low for structures recorded by DLW as well as by interference [14], [16], [32]. Therefore, the actual values of  $a$ ,  $L$ , and  $c$  are most likely very close to the design values. On the other hand, the diameter of the spiral arms is controlled indirectly by the selection of optical exposure level during the fabrication. Setting the laser pulse energy of about 0.7 nJ (measured at the focus), and the distance between the nearest exposure spots along the spiral arm directions of 50 nm usually results in thin, but well cross-linked and mechanically stable SU-8 features. Fig. 3. shows the SEM image of an SU-8 template fabricated under identical conditions as the templates which were subsequently inverted (and therefore could not be imaged by the SEM). The templates have size of  $49 \times 49 \mu\text{m}^2$  (comprising  $49 \times 49$  lattice periods) in the  $y$ - $y$  plane and height of  $10.72 \mu\text{m}$  (comprising eight lattice periods)

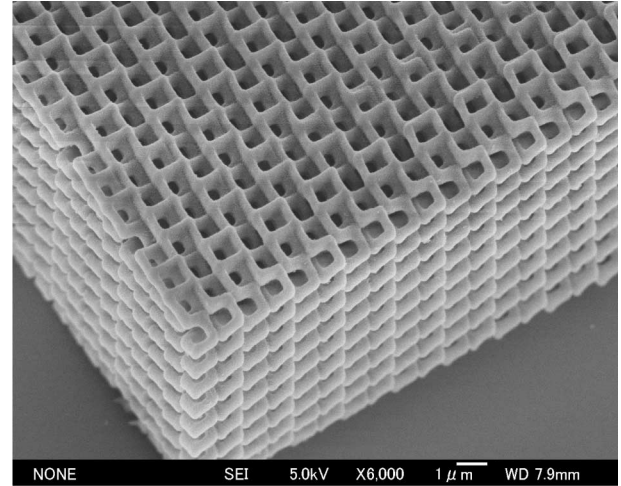


Fig. 3. SEM micrograph of a square spiral photonic template made by direct laser writing in SU8. The direct laser writing was carried out using 800 nm/150 fs pulses at 20-Hz repetition rate focused with an objective lens of numerical aperture  $NA = 1.35$ .

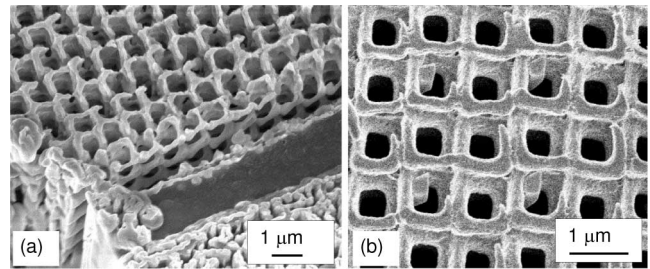


Fig. 4. SEM images of silicon square spiral structure after the double infiltration of SU-8 template. (a) Perspective view showing side-wall cut by FIB milling. (b) Top view detailed image of the top surface of the sample.

along the  $z$ -axis direction. The SEM image gives evidence of the high structural quality achieved, and the absence of visible distortions.

To gain insight into the quality of the infiltrated silicon spirals, several templates were infiltrated using the full sequence of steps from (1) to (6) outlined in Fig. 1(b). The resulting silicon spiral structures allowed inspection by the SEM. Fig. 4 shows the SEM images of silicon spirals in air. In order to inspect the internal morphology of the samples, cutting by focused ion beam (FIB) was used. Cross section of the structure, seen in the FIB cut in Fig. 4(a), demonstrates that internal regions are infiltrated evenly and retain periodicity of the original template. A closer view at the top surface of the sample allows to make an approximate estimate of the lateral spiral arm diameter,  $d_{x,y} = 0.2\text{--}0.25 \mu\text{m}$ . This value will be used in the analysis of the optical properties next. The SEM image also reveals some roughness of the silicon surface and random defects, which may degrade optical quality of the samples.

#### B. Optical Properties of Silicon Square Spiral Structures

Optical properties of the samples were evaluated by reflection measurements at infrared wavelengths. The measurements were

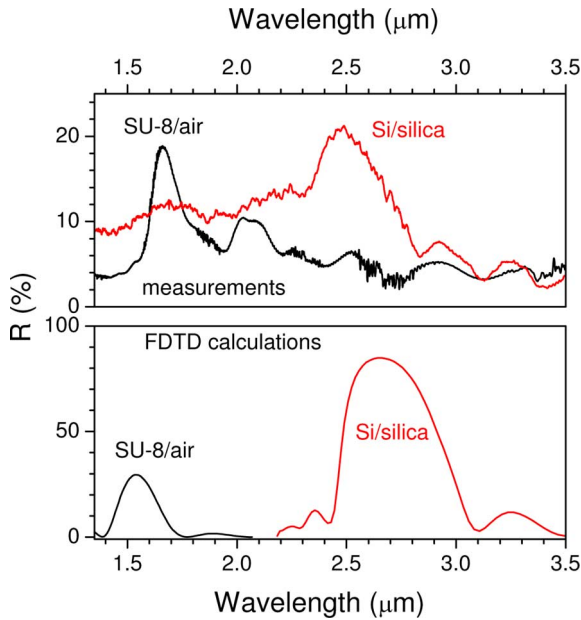


Fig. 5. Reflection spectra of the 3-D spiral template of SU-8 before and after its infiltration by silicon. The top panel shows experimental spectra, while the bottom panel shows spectra simulated by the FDTD technique.

performed using Fourier-transform infrared (FTIR) spectrometer equipped with an infrared microscope attachment (FT/IR-6000TM-M, from Jasco). The use of microscope is convenient for the performance of measurements on small-sized (down to a few micrometers) samples or regions. During the measurements, the samples were mounted with substrate plane perpendicular to the optical axis of the infrared microscope. Hence, reflectivity of the samples was nominally probed along the  $z$ -axis direction, as defined in Fig. 1(a). This direction coincides with the  $\Gamma - Z$  direction in the reciprocal (wave vector) space. However, the infrared microscope uses a Cassegrainian reflection objective with minimum and maximum acceptance angles of  $\alpha_{\min} = 16^\circ$  and  $\alpha_{\max} = 32^\circ$ , respectively. Thus, probing of the reflectivity is actually performed along a range of directions falling into a hollow cone defined by the aforesaid given angles. This circumstance is important for the proper interpretation of the measured optical spectra and their comparison with simple theoretical calculations.

Fig. 5 shows the reflection spectra of the original SU-8 template, and of the sample obtained from this template by double infiltration of silicon (without removal of the intermediate silica matrix). The original template exhibits a reflection peak centered at the wavelength of  $\lambda_c = 1.65 \mu\text{m}$  and having the magnitude of about 20%. Previous studies of the optical properties of various SU-8 templates [14], [16], [17], [18], [33], and the fact that monolithic SU-8 has no significant resonant absorption features at similar wavelengths clearly demonstrate that new reflectance bands should be attributed to photonic stop gaps (PSG) opened due to periodic structuring of SU-8. Infiltration of silicon induces a red-shift of the PSG region from 1.65 to 2.5  $\mu\text{m}$  due to the increase in the average refractive index of the structure and resulting decrease in the photonic band energies.

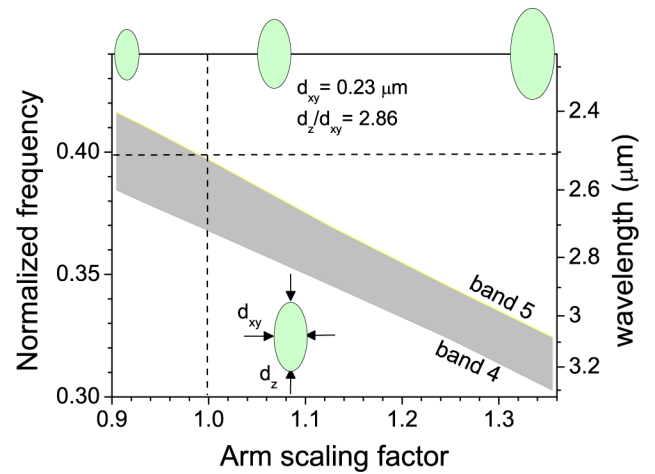


Fig. 6. Photonic stop gap map, or dependence of the stop gap spectral range on the relative proportional scaling factor of the spiral arm cross section for a silicon square spiral structure embedded in silica glass. The arm cross section scaling factor,  $f_{as}$ , is defined with respect to the base cross section having elliptical shape with minor and major diameters  $d_{xy} = 0.23 \mu\text{m}$ , and  $d_z = 2.8 \times d_{xy} = 0.65 \mu\text{m}$ , respectively (for  $f_{as} = 1$ ). The factor  $f_{as}$  is schematically shown as a cross section on the top of the figure and it defines the filling fraction by silicon. The dashed lines emphasize the central wavelength of the reflectance peak in the experimental data (Fig. 5).

The reflectance peak retains its magnitude, but becomes significantly broadened, most likely due to the random scattering by random local variations in the degree of infiltration, aperiodic defects, and rough silicon surface. The same figure also shows theoretical reflectance spectra of both structures calculated using finite-difference time-domain (FDTD) technique. The calculations were performed assuming plane wave propagation along the  $z$ -axis direction. Refractive index values and parameters of the structures were assumed to be close to those of the actual structures:  $n_{\text{Si}} = 3.4$ ,  $n_{\text{SiO}_2} = 1.47$ ,  $a = 1.0 \mu\text{m}$ ,  $L = 1.0 \mu\text{m}$ , and height of the structure equal to eight vertical spiral periods. In Section II-A, we have stressed that diameters of the silicon spiral arms could not be determined directly. One estimate inferred from the SEM image in Fig. 4 gives the range of  $d_{xy} = 0.2\text{--}0.25 \mu\text{m}$ . Vertical diameter of the spiral arm is inherently fixed to  $d_{xy}$  as  $d_z \approx 2.8d_{xy}$  (see the following text). Therefore we treat  $d_{xy}$  as an adjustable parameter and vary it in the range from 200 to 250  $\mu\text{m}$  for best matching with experimental data. The choice of  $d_{xy}$  will be explained next (see Fig. 6 and the accompanying discussion); the calculated reflectivities in Fig. 5 were obtained assuming  $d_{xy} = 0.23 \mu\text{m}$  and  $d_z = 2.8 \times d_{xy} = 0.65 \mu\text{m}$ . As can be seen, the calculations approximately reproduce the spectral positions of experimental reflectivity peaks, and the spectral red-shift resulting from silicon infiltration. Quantitative disagreements between these data sets, especially the difference in the amplitudes of reflectivity peaks for silicon spiral structures, can be attributed to disorder of the samples and finite angular range of their optical probing during the experiments.

Origin of the reflectance peaks can be explained by comparing the experimental data with theoretically calculated photonic band diagrams of the samples. Crucial features of photonic band dispersion in square spiral structures are well known [7], [8].

Silicon square spiral structures typically open a PBG between fourth and fifth photonic bands. PBG maps for [001]-diamond:1 structures show that PBG wider than 10% (in terms of gap width-to-center ratio) can open for  $L \approx (0.7 - 0.9)a$ ,  $c \approx (1.2 - 2.0)a$ , and  $r \approx (0.1 - 0.3)a$ . Our spiral structures are generally close to the aforesaid given ranges, except for the cross-sectional shape of the spiral arms, which is inherently elongated in the  $z$ -axis direction. The elongation factor can be defined as the ratio between longitudinal and lateral diameters of the ellipsoidal cross section of the spiral arms,  $d_{xy}$  and  $d_z$ , respectively. For the laser beam focusing conditions (namely, NA of the focusing lens) and assuming two-photon absorption as the main optical nonlinear process responsible for the optical exposure of SU-8, the elongation factor  $d_z/d_{xy} \approx 2.8$  can be obtained [34]. Since it is difficult to determine the exact absolute values of  $d_{xy}$  and  $d_z$  in the fabricated structures, at first we have analyzed the spectral position of the PSG between the fourth and fifth photonic bands as a function of proportional scaling of elliptical spiral arms. The result of these calculations is shown in Fig. 6. The arm scaling factor,  $f_{as}$ , is defined with respect to the base cross section having  $d_{xy} = 0.23 \mu\text{m}$ , and  $d_z = 2.8 \times d_{xy} = 0.65 \mu\text{m}$ . This factor defines the filling fraction of silicon in the structure for the constant elongation factor of 2.8 determined by the focusing optics, as discussed earlier. The spectral position is indicated in the plot using a dimensionless normalized frequency ( $\omega a/2\pi$ ), and a wavelength for  $a = 1.0 \mu\text{m}$ . As can be seen, the stop gap becomes red-shifted with a scaling factor due to the increasing high-index material filling fraction. The stop-gap wavelength is close to the experimental observation in Fig. 5 when the arm scaling factor approaches unity. Thus, it can be assumed that actual diameters of the silicon spiral arms are  $d_{xy} = 0.23 \mu\text{m}$ , and  $d_z = 0.65 \mu\text{m}$ . Indeed, the value of  $d_{xy}$  is close to that inferred from the SEM observation in Fig. 4. The value of  $d_{xy}$  was estimated from the aforesaid analysis and used in the FDTD reflectance calculations.

Detailed photonic band diagrams for a silicon square spiral structure embedded in silica glass and for as-fabricated SU-8 structure in air are shown in Fig. 7(a) and (b), respectively. The band diagrams (and the gap maps in the previous figure) were calculated by a plane-wave technique implemented in a freely available MIT Photonic Bands software package [35]. The silicon PhC structure has numerous PSGs of considerable spectral width along various directions. Unfortunately, these stop gaps do not merge into a single, omnidirectional PBG. Since most of the parameters of the PhC are close to the optimum ranges suggested in the literature [7], the main reason preventing opening of the PBG in our structures is elliptical elongation of the spiral arms. For comparison, the initial SU-8 template [Fig. 7(b)], whose refractive index contrast is much lower than that of the silicon structure, has even fewer and spectrally narrower PSGs.

The aforesaid data demonstrate that, besides the need to achieve a higher structural quality of the samples, practical application of the fabricated spiral structures in the optical communications spectral range (around  $1.5\text{-}\mu\text{m}$  wavelength) would require to downscale the PhC lattice period by approximately

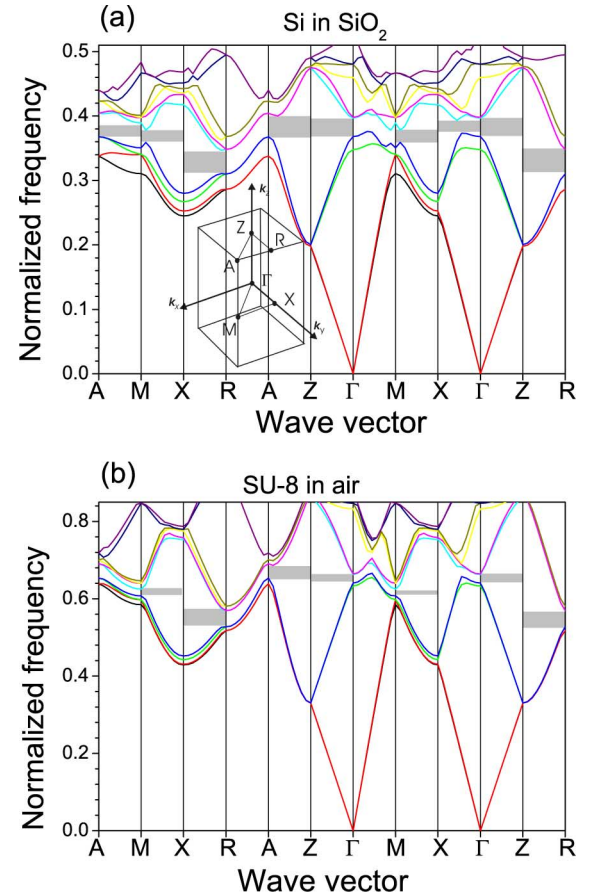


Fig. 7. Photonic band diagram for a silicon square spiral structure embedded in (a) silica glass, and (b) initial “bare” SU-8 template in air. See text for the details. Photonic stop gaps along various directions in the reciprocal space are emphasized by gray-shaded boxes.

40%. Drawing of downscaled structures is technically easily achievable, since the 3-D translation stage has accuracy of a few nanometers. The difficulty, however, is that laser pulse energy must be at the same time reduced by a precisely defined amount necessary in order to produce smaller cross section of the spiral arms. In these circumstances, laser intensity fluctuations is the main factor limiting the resolution of nonlinear laser writing technique, and making the required downscaling difficult at the present moment. More studies are necessary in order to reach the optical telecommunications spectral range.

### C. Holographic Recording by Ultrashort Pulses Using Two-Photon Absorption

Interference recording of 3-D periodic structures by a nonlinear two/multiphoton absorption with high spatial resolution using femtosecond lasers is important for further development of the PhC templating techniques. Recent theoretical investigations have demonstrated the possibility to generate 3-D multiple-beam interference patterns, which, if successfully recorded in SU-8 or other photoresist, may serve as templates for 3-D photonic crystal structures featuring a spectrally wide PBG [20]. These discoveries open a venue for fast and relatively simple

mass-production of semiconductor-based 3-D PhC structures. However, the required templating is a challenging task. First of all, in order to gain the resolution, and to produce periodic interference patterns having a cubic unit cell (i.e., without elongation) comprised of spherically-symmetrical volume elements, one must increase the mutual angles between the interfering beams. At the same time, the optical path difference between the beams must not exceed the pulse duration. While the use of DBS and focusing by a single lens can automatically ensure the optimum spatiotemporal overlap between laser pulses [36]–[39], such a setup cannot increase the interference angles beyond the limitation imposed by the critical angle for total internal reflection [40],  $\alpha_c = \arcsin(1/n) \simeq 38.7^\circ$  for materials with a refractive index of  $n = 1.6$ . On the other hand, use of specially tailored prisms attached to the surface of the sample relaxes the critical angle limitation and allows one to obtain large mutual angles between the beams. Such an approach was instrumental for the recording of periodic structures with face-centered cubic lattice symmetry in SU-8. Symmetric unit cell and spherical symmetry of the “atomic” base element of thus generated interference pattern resulted in PSG at visible wavelengths [25], [26]. However, the fabrication used much longer, nanosecond pulses at ultraviolet wavelengths [25], [27]. Use of ultrashort laser pulses and exploitation of optical exposure via nonlinear absorption (TPA) using a similar optical setup is still a daunting task. Next, we demonstrate an attempt to combine all of the required factors (large interference angle, short-period interference pattern, use of ultrafast laser pulses for the exploitation of nonlinear absorption) in practice. We describe the adjustment of spatiotemporal overlap between the pulses and recording of a simple 2-D structure.

The setup used for the four-beam interference recording was described earlier in Section II-D and Fig. 2(b). Spatiotemporal overlap between the four pulses was adjusted using PL from coumarin dye solution, excited via two-photon absorption and imaged by a CCD camera, as illustrated in Fig. 2(c). The alignment of optical paths was optimized for pairs of the interfering beams. Fig. 8 shows PL images corresponding to various stages of the alignment. Only the central parts of the images, emphasized by the circles are important; the linear and cross-like bright regions result from the PL guided by the higher-index cover glass substrates. The regions of strongest nonlinear PL correspond to perfect temporal coincidence between the pulses. Fig. 8 illustrates the alignment sequence of two, three, and four beams. Time delay between the pairs of beams can be visualized as spatial separation between the PL maxima, as shown in Fig. 8. Experimentally, the temporal coincidence was assessed with accuracy better than  $5 \mu\text{m}$  in the units of path length, whereas the 150-fs long pulse corresponds to a  $45\text{-}\mu\text{m}$  path length. The maximum PL corresponded to the shortest pulses on the sample. Once all the beams are collected to the same focal volume at the same time, a pulse prechirping was carried out by monitoring the PL intensity for the highest irradiance.

During the recording, the SU-8 sample was positioned in the region of the interference pattern. Fig. 9(a) shows a 2-D square pattern of rods recorded by four-beam interference. The lattice period of 410 nm is close to the expected value of  $a =$

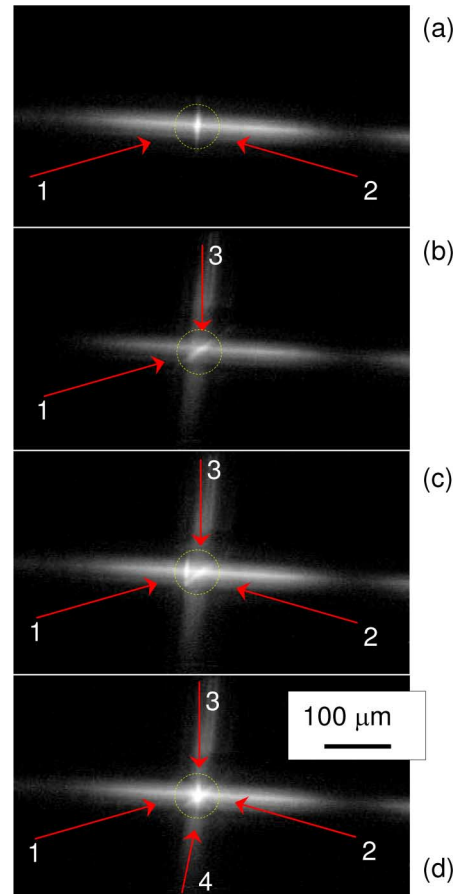


Fig. 8. Photoluminescence images of coumarin dye solution taken during temporal adjustment of the (a) pair of horizontally aligned beams 1–2, and the pair of vertically aligned beams 1–3 (b). The spatial region of vanishing time delay is emphasized by the circle and has a width of approximately  $13 \mu\text{m}$ . In (a), the zero delay  $\Delta t_{12} = 0 \text{ fs}$  is apparent by the vertical line of high-intensity PL. (c) An example of poor timing between the beams 1, 2, and 3; the spatial separation of strongest PL regions is apparent. The width of the time coincidence zone is approximately  $13 \mu\text{m}$ .

$\lambda/(\sqrt{2} \sin \theta) \simeq 401 \pm 3 \text{ nm}$ . Here,  $\theta = 70^\circ$  is the mutual angle in the pairs of beams and  $\lambda = 800/1.5 \text{ nm}$  is the laser pulse wavelength. The uncertainty range corresponds to  $\Delta\theta = \pm 1^\circ$ . Fourier transform of the image of recorded pattern shown in Fig. 9(b) corroborates the square geometry. Elliptical shapes of the rods are most probably caused by misalignment of the beams. For two-beam interference (not shown) 2-D gratings with a period of 280 nm were obtained. This value is close to the theoretical estimate  $a = \lambda/(2 \sin \theta) = 284 \text{ nm}$ .

The achieved alignment and optical recording by subpicosecond laser pulse interference indicates the possibility to further develop the experimental setup by employing different incidence angles for different beams and increasing the number of beams to five or even more. Especially important is the inclusion of a central beam that can be coupled to the sample through the flat top of the prism thus allowing one to obtain 3-D structures with cubic lattice symmetry, similar as in the previous studies that used much longer pulses [25]. In principle, all of the 14 3-D Bravais lattices can be generated by interference of four noncoplanar beams [41]. Moreover, phase control of the beams

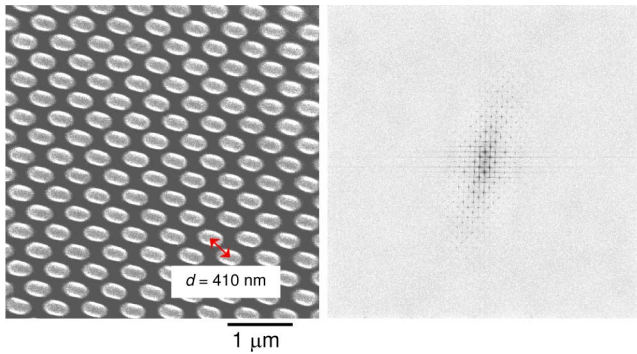


Fig. 9. SEM image of 2-D structure recorded by (a) four-beam interference, and (b) Fourier transform of the obtained pattern. The lattice period  $a = 410 \pm 5$  nm; the structure height  $h = 3 \mu\text{m}$ , the exposure time 30 s, the total incident pulse energy is  $4 \times 15 \mu\text{J}$ , the pulse repetition rate is 1 kHz.

can be utilized to create patterns of more complex and transitional geometries [42], [43]. Realization of such templates is currently under investigation. The space-time collection of several ultrashort pulses at arbitrary large angles of incidence on the areas of millimeter cross sections for 3-D recording of PhC templates with the same lateral and axial periods appears technically achievable. Only the nonlinear, e.g., two or multiphoton absorption can deliver 3-D structuring of photopolymers and is highly required for the practical fabrication of 3-D PhC-based devices.

#### IV. CONCLUSION

We have reported femtosecond direct laser writing of PhC templates in a commercial photoresist SU-8, their replication with silicon by double inversion, and presented analysis of structural and optical properties of the obtained silicon square spiral PhC structures. These structures were found to exhibit good structural periodicity and to have photonic stop gaps centered at the wavelength of  $2.5 \mu\text{m}$ . This result is inferred from theoretical calculations of photonic bands and optical reflectivity spectra. The composite Si-SiO<sub>2</sub> structures apparently do not have PBGs due to the elliptical elongation of the spiral arms. Further studies are needed in order to determine whether this limitation can be overcome by additional structural tailoring of SU-8 templates. Band structure calculations suggest that a complete PBG exists when the sacrificial SiO<sub>2</sub> component is removed. Finally, we have investigated multibeam two-photon absorption lithography as an alternative to the serial direct laser writing process. The optical setup for high-resolution laser lithography using ultrafast pulses was described and recording of simple 2-D structures was demonstrated.

#### REFERENCES

[1] E. Yablonovitch, "Inhibited spontaneous emission in solid-state physics and electronics," *Phys. Rev. Lett.*, vol. 58, pp. 2059–2062, 1987.  
 [2] S. John, "Strong localization of photons in certain disordered dielectric superlattices," *Phys. Rev. Lett.*, vol. 58, no. 23, pp. 2486–2489, 1987.  
 [3] S. Noda, K. Tomoda, N. Yamamoto, and A. Chutinan, "Full three-dimensional photonic bandgap crystals at near-infrared wavelengths," *Science*, vol. 289, no. 5479, pp. 604–606, 2000.

[4] S. Noda, "Three-dimensional photonic crystals operating at optical wavelength region," *Physica B*, vol. 279, pp. 142–149, 2000.  
 [5] M. Qi, E. Lidorikis, P. Rakich, S. Johnson, J. Joannopoulos, E. Ippen, and H. Smith, "A three-dimensional optical photonic crystal with designed point defects," *Nature*, vol. 429, no. 6991, pp. 538–542, 2004.  
 [6] A. Blanco, E. Chomski, S. Grabtchak, M. Ibisate, S. John, S. Leonard, C. Lopez, F. Meseguer, H. Miguez, J. Mondia, G. Ozin, O. Toader, and H. van Driel, "Large-scale synthesis of a silicon photonic crystal with a complete three-dimensional bandgap near 1.5 micrometres," *Nature*, vol. 405, no. 6785, pp. 437–440, 2000.  
 [7] O. Toader and S. John, "Square spiral photonic crystals: Robust architecture for microfabrication of materials with large three-dimensional photonic band gaps," *Phys. Rev. E, Stat. Phys. Plasmas Fluids Relat. Interdiscip. Top.*, vol. 66, pp. 016610-1–016610-18, 2002.  
 [8] O. Toader and S. John, "Proposed square spiral microfabrication architecture for large three-dimensional photonic band gap crystals," *Science*, vol. 292, pp. 1133–1135, 2001.  
 [9] M. Jensen and M. Brett, "Square spiral 3D photonic bandgap crystals at telecommunications frequencies," *Opt. Express*, vol. 13, pp. 3348–3354, 2005.  
 [10] S. Kennedy, M. Brett, H. Miguez, O. Toader, and S. John, "Optical properties of a three-dimensional silicon square spiral photonic crystal," *Photon. Nanostruct.*, vol. 1, pp. 37–42, 2003.  
 [11] S. Kennedy, M. Brett, O. Toader, and S. John, "Fabrication of tetragonal square spiral photonic crystals," *Nano Lett.*, vol. 2, pp. 59–62, 2002.  
 [12] D.-X. Ye, Z.-P. Yang, A. Chang, J. Bur, S. Lin, T.-M. Lu, R. Z. Wang, and S. John, "Experimental realization of a well-controlled 3d silicon spiral photonic crystal," *J. Phys. D, Appl. Phys.*, vol. 40, pp. 2624–2628, 2007.  
 [13] A. Chutinan and S. Noda, "Spiral three-dimensional photonic-band-gap structure," *Phys. Rev. B, Condens. Matter*, vol. 57, pp. R2006–R2008, 1998.  
 [14] V. Mizeikis, K. Seet, S. Juodkazis, and H. Misawa, "Three-dimensional woodpile photonic crystal templates for the infrared spectral range," *Opt. Lett.*, vol. 29, no. 17, pp. 2061–2063, 2004.  
 [15] H. Sun, S. Matsuo, and H. Misawa, "Three-dimensional photonic crystal structures achieved with two-photon-absorption photopolymerization of resin," *Appl. Phys. Lett.*, vol. 74, pp. 786–788, 1999.  
 [16] K. Seet, V. Mizeikis, S. Matsuo, S. Juodkazis, and H. Misawa, "Three-dimensional spiral-architecture photonic crystals obtained by direct laser writing," *Adv. Mater.*, vol. 17, no. 5, pp. 541–545, 2005.  
 [17] K. Seet, V. Mizeikis, S. Juodkazis, and H. Misawa, "Spiral three-dimensional photonic crystals for telecommunications spectral range," *Appl. Phys. A, Solids Surf.*, vol. 82, pp. 683–688, 2006.  
 [18] K. K. Seet, V. Mizeikis, S. Juodkazis, and H. Misawa, "Three-dimensional circular spiral photonic crystals structures recorded by femtosecond pulses," *J. Non-Cryst. Solids*, vol. 352, pp. 2390–2394, 2006.  
 [19] S. Juodkazis, V. Mizeikis, K. K. Seet, M. Miwa, and H. Misawa, "Two-photon lithography of nanorods in SU-8 photoresist," *Nanotechnology*, vol. 16, pp. 846–849, 2005.  
 [20] T. Chan, O. Toader, and S. John, "Photonic band gap templating using optical interference lithography," *Phys. Rev. E, Stat. Phys. Plasmas Fluids Relat. Interdiscip. top.*, vol. 71, pp. 046605-1–046605-18, 2005.  
 [21] O. Toader, T. Chan, and S. John, "Photonic band gap architectures for holographic lithography," *Phys. Rev. Lett.*, vol. 92, p. 043905, 2004.  
 [22] T. M. Chan, O. Toader, and S. John, "Photonic band-gap formation by optical-phase-mask lithography," *Phys. Rev. E, Stat. Phys. Plasmas Fluids Relat. Interdiscip. top.*, vol. 73, pp. 046610-1–046610-11, 2006.  
 [23] N. Tétreault, G. von Freymann, M. Deubel, M. H. F. Pérez-Willard, S. John, M. Wegener, and G. A. Ozin, "New route to three-dimensional photonic bandgap materials: Silicon double inversion of polymer templates," *Adv. Mater.*, vol. 18, no. 4, pp. 457–460, 2006.  
 [24] A. Ledermann, L. Cademartiri, M. Hermatschweiler, C. Toninelli, G. Ozin, D. Wiersma, M. Wegener, and G. von Freymann, "Three-dimensional silicon inverse photonic quasicrystals for infrared wavelengths," *Nat. Mater.*, vol. 5, pp. 942–945, 2006.  
 [25] Y. V. Miklyaev, D. C. Meisel, A. Blanco, G. von Freymann, K. Busch, W. Koch, C. Enkrich, M. Deubel, and M. Wegener, "Three-dimensional face-centered-cubic photonic crystal templates by laserholography: Fabrication, optical characterization, and band-structure calculations," *Appl. Phys. Lett.*, vol. 82, pp. 1284–1285, 2003.  
 [26] Y. K. Pang, J. C. W. Lee, H. F. Lee, W. Y. Tam, and C. T. C. P. Sheng, "Chiral microstructures (spirals) fabrication by holographic lithography," *Opt. Express*, vol. 13, no. 19, pp. 7615–7620, 2005.

- [27] R. C. Rumpf and E. G. Johnson, "Fully three-dimensional modeling of the fabrication and behavior of photonic crystals formed by holographic lithography," *J. Opt. Soc. Amer. A, Opt. Image Sci.*, vol. 21, pp. 1703–1713, 2004.
- [28] M. Maldovan and E. Thomas, "Diamond-structured photonic crystals," *Nat. Mater.*, vol. 3, pp. 593–600, 2004.
- [29] S. Juodkakis, S. Matsuo, H. Misawa, V. Mizeikis, A. M. H. B. Sun, Y. Tokuda, M. Takahashi, T. Yoko, and J. Nishii, "Application of femtosecond laser pulses for microfabrication of transparent media," *Appl. Surf. Sci.*, vol. 197–198, pp. 705–709, 2002.
- [30] G. Witzgall, R. Vrijen, E. Yablonovitch, V. Doan, and B. Schwartz, "Single-shot two-photon exposure of commercial photoresist for the production of three-dimensional structures," *Opt. Lett.*, vol. 23, pp. 1745–1747, 1998.
- [31] K. Seet, S. Juodkakis, V. Jarutis, and H. Misawa, "Feature-size reduction of photopolymerized structures by femtosecond optical curing of SU-8," *Appl. Phys. Lett.*, vol. 89, p. 24106, 2006.
- [32] T. Kondo, S. Juodkakis, and H. Misawa, "Reduction of capillary force for high-aspect ratio nanofabrication," *Appl. Phys. A, Solids Surf.*, vol. 81, no. 8, pp. 1583–1586, 2005.
- [33] K. Seet, V. Mizeikis, S. Juodkakis, and H. Misawa, "Three-dimensional horizontal circular spirals photonic crystals with stopgaps below  $1\ \mu\text{m}$ ," *Appl. Phys. Lett.*, vol. 88, pp. 221101-1–221101-3, 2005.
- [34] M. Gu, *Advanced Optical Imaging Theory* (Springer Series in Optical Sciences 75). New York: Springer-Verlag, 1999.
- [35] S. Johnson and J. Joannopoulos, "Block-iterative frequency-domain methods for Maxwell's equations in a planewave basis," *Opt. Express*, vol. 8, no. 3, pp. 173–190, 2001.
- [36] A. A. Maznev, T. F. Crimmins, and K. A. Nelson, "How to make femtosecond pulses overlap," *Opt. Lett.*, vol. 23, pp. 1378–1380, 1998.
- [37] T. Kondo, S. Matsuo, S. Juodkakis, and H. Misawa, "A novel femtosecond laser interference technique with diffractive beam splitter for fabrication of three-dimensional photonic crystals," *Appl. Phys. Lett.*, vol. 79, no. 6, pp. 725–727, 2001.
- [38] T. Kondo, S. Matsuo, S. Juodkakis, V. Mizeikis, and H. Misawa, "Multiphoton fabrication of periodic structures by multibeam interference of femtosecond pulses," *Appl. Phys. Lett.*, vol. 82, no. 17, pp. 2758–2760, 2003.
- [39] T. Kondo, S. Juodkakis, V. Mizeikis, H. Misawa, and S. Matsuo, "Holographic lithography of periodic two- and three-dimensional microstructures in photoresist SU-8," *Opt. Express*, vol. 14, no. 17, pp. 7943–7953, 2006.
- [40] M. Campbell, D. N. Sharp, M. T. Harrison, R. G. Denning, and A. Turberfield, "Fabrication of photonic crystals for the visible spectrum by holographic lithography," *Nature*, vol. 404, no. 6773, pp. 53–56, 2000.
- [41] L. Z. Cai, X. L. Yang, and Y. R. Wang, "All fourteen Bravais lattices can be formed by interference of four non-coplanar beams," *Opt. Lett.*, vol. 27, pp. 900–902, 2002.
- [42] T. Kondo, S. Matsuo, S. Juodkakis, V. Mizeikis, and H. Misawa, "Three-dimensional recording by femtosecond pulses in polymer materials," *J. Photopolym. Sci. Tech.*, vol. 16, no. 3, pp. 427–432, 2003.
- [43] T. Kondo, S. Juodkakis, V. Mizeikis, S. Matsuo, and H. Misawa, "Fabrication of three-dimensional periodic microstructures in photoresist SU-8 by phase-controlled holographic lithography," *New J. Phys.*, vol. 8, pp. 250–265, 2006.



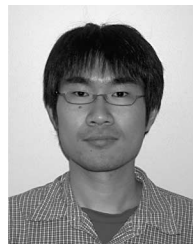
**Kock Khuen Seet** received the Bachelor's degree in computer science from Kyushu University, Fukuoka, Japan, in 1994, and the Ph.D. degree in electronics and information engineering from the Graduate School of Engineering, Hokkaido University, Sapporo, Japan (2006).

He is currently with Hitachi High-Technologies, Tokyo, Japan. His past research interests include fabrication and characterization of nanostructures known as photonic crystals using direct laser writing in photoresist. His current research interests include the development of critical dimension scanning electron microscope system for semiconductor manufacturing.



**Vygantas Mizeikis** received the Diploma and the Ph.D. degrees in physics from Vilnius University, Vilnius, Lithuania, in 1989 and 1997, respectively.

From 1997 to 2000, he was a Researcher at Vilnius University. He subsequently moved to Japan, where he was a Postdoctoral Researcher at the University of Tokushima during 2000–2003. Since 2003, he has been with Hokkaido University, Sapporo, Japan, where he is currently a Postdoctoral Researcher at the Research Institute for Electronic Science. He is the author or coauthor of more than 40 scientific papers in ISI journals. His current research interests include optical fabrication and characterization of photonic crystal structures, plasmonics, and photomodification of materials by ultrafast laser pulses.



**Kenta Kannari** received the B.Sc. degree from the Faculty of Electrical Engineering, Hokkaido University, Sapporo, Japan, in 2006, where he is currently working toward the Master's degree. His current research interests include fabrication of photonic crystals by multibeam interference with phase control using femtosecond pulses.



**Saulius Juodkakis** received the Diploma in Physics from Vilnius University, Vilnius, Lithuania, in 1986, and the Ph.D. degree in physics and material science jointly from Vilnius University and l'Université Claude Bernard of Lyon, Lyon, France, in 1997.

During 1997–2000, he was a postdoctoral researcher at Tokushima University, Tokushima, Japan, where he was engaged in research on nitride photonic semiconductor and photonic nanomaterials. He became an Assistant Professor at the Tokushima University in 2000 and joined Hokkaido University, Sapporo, Japan, in 2004, where he is currently an Associate Professor at the Research Institute for Electronic Science. He is the author or coauthor of more than 100 scientific papers in ISI journals. His current research interests include light-matter interactions in the microdomain, plasmonics, laser tweezers, and applications of ultrafast laser pulses.



**Hiroaki Misawa** received the B.Sc. degree in engineering from the Department of Engineering, Tokyo Metropolitan University, Tokyo, Japan, in 1979, and the M.Sc. degree in engineering and the Ph.D. degree in chemistry from the University of Tsukuba, Tsukuba, Japan, in 1981 and 1984, respectively.

After postdoctoral positions at the Universities of Texas and Tsukuba and an assistant professorship at the University of Tsukuba, he joined the Microphotoconversion Project at the Exploratory Research for Advanced Technology (ERATO), Japan Science & Technology Agency (JST). He became an Associate Professor in the Department of Engineering, Tokushima University, in 1993, and became a Full Professor in 1995. He then moved on to Hokkaido University, Sapporo, Japan, as a Full Professor in 2003. He is currently a Professor at the Research Institute for Electronic Science and Head of the Nanotechnology Research Center at Hokkaido University. He is the author or coauthor of more than 200 papers published in international journals. His current research interests include photochemistry, light-matter interaction, ultrafast processes in materials, photonic crystals, and plasmonics.



**Nicolas Tétreault** received the Ph.D. degree in physical chemistry from the University of Toronto, ON, Canada, in 2005.

He is currently an Associate Researcher at the Nanoscience Centre and the Cavendish Laboratories at the University of Cambridge, Cambridge, U.K. He participated in multiple international research projects. He is the author or coauthor of more than 20 papers published in international journals. His current research interests include the fabrication of novel photonic and optoelectronic materials for photo-

voltaic, communication, and optical computing applications.

Dr. Tétreault was the recipient of the Gold Medal of the Governor General for his achievements in material science in general and in 3-D photonic crystals in particular.



**Sajeef John** received the Bachelor's degree in physics from the Massachusetts Institute of Technology, Cambridge, in 1979, and the Ph.D. degree in physics from Harvard University, Cambridge, MA, in 1984.

His Ph.D. work at Harvard introduced the theory of classical wave localization, and in particular, the localization of light in 3-D strongly scattering dielectrics. From 1984 to 1986, he was a Natural Sciences and Engineering Research Council of Canada Postdoctoral Fellow at the University of Pennsylvania

as well as a Laboratory Consultant to the Corporate Research Science Laboratories of Exxon Research and Engineering during 1985–1989. From 1986 to 1989, he was an Assistant Professor of Physics at Princeton University, Princeton, NJ. While at Princeton, he developed the concept of photonic band gap materials, providing a systematic route to his original conception of the localization of light. He was a Laboratory Consultant to Bell Communications Research, Red Bank, NJ, in 1989. In the fall of 1989, he joined the senior physics faculty at the University of Toronto, Toronto, ON, Canada. He has been a Principal Investigator for Photonics Research Ontario, a Canadian center of excellence. He is currently a University Professor at the University of Toronto and Government of Canada Research Chair holder.

Prof. John is a Fellow of the Canadian Institute for Advanced Research.